

Finite Element solution of the fiber/matrix interface crack problem: convergence properties and mode mixity of the Virtual Crack Closure Technique

Luca Di Stasio^{a,b}, Janis Varna^b, Zoubir Ayadi^a

^aUniversité de Lorraine, EEIGM, IJL, 6 Rue Bastien Lepage, F-54010 Nancy, France

^bLuleå University of Technology, University Campus, SE-97187 Luleå, Sweden

Abstract

Priority: 3

Target journal(s): Engineering Fracture Mechanics, Theoretical and Applied Fracture Mechanics, International Journal of Fracture

1. Introduction

Bi-material interfaces represent the basic load transfer mechanism at the heart of Fiber Reinforced Polymer Composite (FRPC) materials. They are present at the macroscale, in the form of adhesive joints; at the mesoscale, as
5 interfaces between layers with different orientations; at the microscale, as fiber-matrix interfaces. Bi-material interfaces have for long attracted the attention of researchers in Fracture Mechanics [1, 2], due to their hidden complexity. The problem was first addressed in the 1950's by Williams [3], who derived through a linear elastic asymptotic analysis the stress distribution around an
10 *open* crack (i.e. with crack faces nowhere in contact for any size of the crack) between two infinite half-planes of dissimilar materials and found the existence of a strong oscillatory behavior in the stress singularity at the crack tip of the form

$$r^{-\frac{1}{2}} \sin(\varepsilon \log r) \quad \text{with} \quad \varepsilon = \frac{1}{2\pi} \log \left(\frac{1-\beta}{1+\beta} \right); \quad (1)$$

in which β is one of the two parameters introduced by Dundurs [4] to characterize bi-material interfaces:

$$\beta = \frac{\mu_2(\kappa_1 - 1) - \mu_1(\kappa_2 - 1)}{\mu_2(\kappa_1 + 1) + \mu_1(\kappa_2 + 1)} \quad (2)$$

where $\kappa = 3 - 4\nu$ in plane strain and $\kappa = \frac{3-4\nu}{1+\nu}$ in plane stress, μ is the shear modulus, ν Poisson's coefficient, and indexes 1,2 refer to the two bulk materials joined at the interface. Defining a as the length of the crack, it was found that the size of the oscillatory region is in the order of $10^{-6}a$ [5]. Given the oscillatory behaviour of the crack tip singularity of the stress field of Eq. 1, the definition of Stress Intensity Factor (SIF) $\lim_{r \rightarrow 0} \sqrt{2\pi r} \sigma$ ceases to be valid as it returns logarithmically infinite terms [1]. Furthermore, it implies that the Mode mixity problem at the crack tip is ill-posed.

It was furthermore observed, always in the context of Linear Elastic Fracture Mechanics (LEFM), that an interpenetration zone exists close to the crack tip [6, 7] with a length in the order of 10^{-4} [6]. Following conclusions firstly proposed in [7], the presence of a *contact zone* in the crack tip neighborhood, of a length to be determined from the solution of the elastic problem, was introduced in [8] and shown to provide a physically consistent solution to the straight bi-material interface crack problem.

The curved bi-material interface crack, more often referred to as the fiber-matrix interface crack (or debond) due to its relevance in FRPCs, was first treated by England [9] and by Perlman and Sih [10], who provided the analytical solution of stress and displacement fields for a circular inclusion with respectively a single debond and an arbitrary number of debonds. Building on their work, Toya [11] particularized the solution and provided the expression of the Energy Release Rate (ERR) at the crack tip. The same problems exposed previously for the *open* straight bi-material were shown to exist also for the *open* fiber-matrix interface crack: the presence of strong oscillations in the crack tip singularity and crack face interpenetration after a critical initial flaw size.¹

¹For the fiber-matrix interface crack, flaw size is measured in terms of the angle $\Delta\theta$ sub-

In order to treat cases more complex than the single partially debonded fiber in an infinite matrix of [9, 10, 11], numerical studies followed. In the 1990's, París and collaborators [12] developed a Boundary Element Method (BEM) with the use of discontinuous singular elements at the crack tip and the Virtual Crack Closure Integral (VCCI) [13] for the evaluation of the Energy Release Rate (ERR). They validated their results [12] with respect to Toya's analytical solution [11] and analyzed the effect of BEM interface discretization on the stress field in the neighborhood of the crack tip [14]. Following Comninou's work on the straight crack [8], they furthermore recognized the importance of contact to retrieve a physical solution avoiding interpenetration [12] and studied the effect of the contact zone on debond ERR [15]. Their algorithm was then applied to investigate the fiber-matrix interface crack under different geometrical configurations and mechanical loadings [16, 17, 18, 19, 20, 21, 22].

Recently the Finite Element Method (FEM) was also applied to the solution of the fiber-matrix interface crack problem [23, 24, 25], in conjunction with the Virtual Crack Closure Technique (VCCT) [26, 27] for the evaluation of the ERR at the crack tip. In [23], the authors validated their model with respect to the BEM results of [12], but no analysis of the effect of the discretization in the crack tip neighborhood comparable to [14] was proposed. Thanks to the interest in evaluating the ERR of interlaminar delamination, different studies exist in the literature on the effect of mesh discretization on Mode I and Mode II ERR of the bi-material interface crack when evaluated with the VCCT in the context of the FEM [28, 29, 30]. However, no comparable analysis can be found in the literature on the application of the VCCT to the fiber-matrix interface crack (circular bi-material interface crack) problem in the context of a linear elastic FEM solution. It is this gap that the present work aims to address. We first present the FEM formulation of the problem, together with the main geometrical characteristics, material properties, boundary conditions and loading. We then propose a vectorial formulation of the VCCT and express

tended by half of the arc-crack, i.e. $a = 2\Delta\theta$.

the Mode I and Mode II ERR in terms of the FEM natural variables. With this tool, we derive an analytical estimate of the ERR convergence and compare it with numerical results.

2. FEM formulation of the fiber-matrix interface crack problem

In order to investigate the fiber-matrix interface crack problem, a 2-dimensional model of a single fiber inserted in a rectangular matrix element is considered (see Figure 1). Total element length and height are respectively $2L$ and L , where L is determined by the fiber radius R_f and the fiber volume fraction V_f by

$$L = \frac{R_f}{2} \sqrt{\frac{\pi}{V_f}}. \quad (3)$$

The fiber radius R_f is assumed to be equal to $1 \mu m$. This choice is not dictated by physical considerations but for simplicity. It is thus useful to remark that, in a linear elastic solution as the one considered in the present work, the ERR is proportional to the geometrical dimensions of the model and, consequently, recalculation of the ERR for fibers of any size requires a simple multiplication.

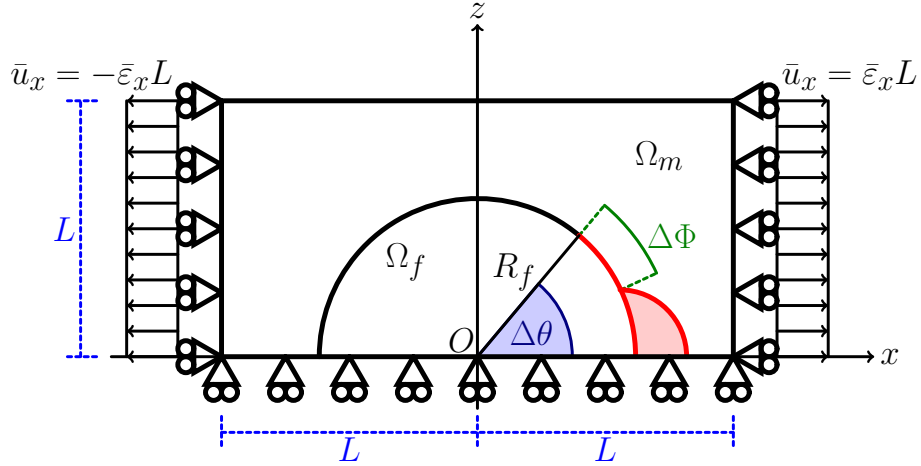


Figure 1: Schematic of the model with its main parameters.

As shown in Fig. 1, the debond is placed symmetrically with respect to the x axis and its size is characterized by the angle $\Delta\theta$ (which makes the full debond size equal to $2\Delta\theta$ and the full crack length equal to $R_f 2\Delta\theta$). A region $\Delta\Phi$ of variable size appears at the crack tip for large debond sizes (at least $\geq 60^\circ - 80^\circ$), in which the crack faces are in contact with each other and free to slide. Frictionless contact is thus considered between the two crack faces to allow free sliding and avoid interpenetration. Symmetry with respect to the x axis is applied on the lower boundary while the upper surface is left free. Kinematic coupling on the x -displacement is applied along the left and right sides of the model in the form of a constant x -displacement $\pm \bar{\epsilon}_x L$, which corresponds to transverse strain $\bar{\epsilon}_x$ equal to 1%.

Table 1: Summary of the mechanical properties of fiber and matrix. E stands for Young's modulus, μ for shear modulus and ν for Poisson's ratio.

Material	E [GPa]	μ [GPa]	ν [-]
Glass fiber	70.0	29.2	0.2
Epoxy	3.5	1.25	0.4

The model problem is solved with the Finite Element Method (FEM) within the Abaqus environment, a commercial FEM software [31]. The model is meshed with second order, 2D, plane strain triangular (CPE6) and rectangular (CPE8) elements. A regular mesh of quadrilateral elements with almost unitary aspect ratio is used at the crack tip. The angular size δ of an element in the crack tip neighborhood represents the main parameter of the numerical analysis. The crack faces are modeled as element-based surfaces and a small-sliding contact pair interaction with no friction is imposed between them. The Mode I, Mode II and total Energy Release Rates (ERRs) (respectively referred to as G_I , G_{II} and G_{TOT}) are evaluated using the VCCT [27], implemented in a in-house Python routine. A glass fiber-epoxy system is considered in the present work, and it is assumed that their response lies always in the linear elastic domain. The material properties of glass fiber and epoxy are reported in Table 1.

3. Vectorial formulation of the Virtual Crack Closure Technique (VCCT)

3.1. Foundational relations

110 In the isoparametric formulation of the Finite Element Method, the element Jacobian J and its inverse J^{-1} can be expressed in general as

$$\underline{\underline{J}} = \begin{bmatrix} \underline{e}_\xi | \underline{e}_\eta \end{bmatrix} = \begin{bmatrix} \frac{\partial x}{\partial \xi} & \frac{\partial x}{\partial \eta} \\ \frac{\partial y}{\partial \xi} & \frac{\partial y}{\partial \eta} \end{bmatrix} \quad \underline{\underline{J}}^{-1} = \begin{bmatrix} \underline{e}^x | \underline{e}^y \end{bmatrix} = \begin{bmatrix} \frac{\partial \xi}{\partial x} & \frac{\partial \xi}{\partial y} \\ \frac{\partial \eta}{\partial x} & \frac{\partial \eta}{\partial y} \end{bmatrix} \quad (4)$$

where $\{e_\xi, e_\eta\}$ and $\{e^x, e^y\}$ are respectively the covariant and contravariant basis vectors of the mapping between global $\{x, y\}$ and local element $\{\xi, \eta\}$ coordinates:

$$\underline{e}_\xi = \begin{bmatrix} \frac{\partial x}{\partial \xi} \\ \frac{\partial y}{\partial \xi} \end{bmatrix} \quad \underline{e}_\eta = \begin{bmatrix} \frac{\partial x}{\partial \eta} \\ \frac{\partial y}{\partial \eta} \end{bmatrix}, \quad (5)$$

$$\underline{e}_x = \begin{bmatrix} \frac{\partial \xi}{\partial x} \\ \frac{\partial \eta}{\partial x} \end{bmatrix} \quad \underline{e}_y = \begin{bmatrix} \frac{\partial \xi}{\partial y} \\ \frac{\partial \eta}{\partial y} \end{bmatrix}. \quad (6)$$

115 Denoting by d the number of geometrical dimensions of the problem ($d = 2$ in the present work) and by \underline{p} the $d \times 1$ position vector in global coordinates, we can formally introduce the $3(d-1) \times d$ matrix operator of partial differentiation $\underline{\underline{\tilde{B}}}$ such that

$$\underline{\varepsilon}(\underline{p}) = \underline{\underline{\tilde{B}}} \cdot \underline{u}(\underline{p}), \quad (7)$$

120 where \underline{u} and $\underline{\varepsilon}$ are respectively the $d \times 1$ displacement vector and the $3(d-1) \times 1$ strain vector in Voigt notation. Denoting by n the number of nodes of a generic element ($n = s \times m$ where s represents the number of sides of the element and m the order of the shape functions), we can furthermore introduce the $d \times d \cdot n$ matrix $\underline{\underline{N}}$ of shape functions such that

$$\underline{u} = \underline{\underline{N}} \cdot \underline{u}_N, \quad (8)$$

where \underline{u}_N is the $d \cdot n \times 1$ vector of element nodal variables. Having intro-
125 duced $\underline{\tilde{B}}$ and \underline{N} in Equations 7 and 8 respectively, it is possible to define the
 $3(d-1) \times d \cdot n$ matrix \underline{B} of derivatives (with respect to global coordinates) of
shape functions as

$$\underline{B} = \underline{\tilde{B}} \cdot \underline{N}. \quad (9)$$

We introduce the linear elastic material behavior in the form of the $3(d-1) \times$
 $3(d-1)$ rigidity matrix \underline{D} such that

$$\underline{\sigma} = \underline{D} \cdot \underline{\varepsilon}, \quad (10)$$

130 where $\underline{\sigma}$ the $3(d-1) \times 1$ stress vector in Voigt notation. It is finally possible
to define the $n \times n$ element stiffness matrix \underline{k}_e as

$$\underline{k}_e = \int_{V_e(x,y)} (\underline{B}^T \underline{D} \cdot \underline{B}) dV_e(x, \dots, y) = \int_{V_e(\xi,\eta)} (\underline{B}^T \underline{D} \cdot \underline{B}) \sqrt{g} dV_e(\xi, \dots, \eta), \quad (11)$$

where $g = \det(\underline{J}^T \underline{J})$ and V_e is the element volume. Given that isoparametric
elements are always defined between -1 and 1 in each dimension, Equation 11
can simplified to

$$\underline{k}_e = \int_{-1}^1 \dots \int_{-1}^1 (\underline{B}^T \underline{D} \cdot \underline{B}) \sqrt{g} d\xi, \dots, d\eta, \quad (12)$$

135 which is amenable to numerical integration by means of a Gaussian quadra-
ture of the form

$$\underline{k}_e \approx \sum_{i=1}^N \dots \sum_{j=1}^N w_i \dots w_j (\underline{B}^T(\xi_i, \dots, \eta_j) \cdot \underline{D} \cdot \underline{B}(\xi_i, \dots, \eta_j) \sqrt{g}), \quad (13)$$

where (ξ_i, \dots, η_j) are the coordinates of the N Gaussian quadrature points.
The element stiffness matrix as evaluated in Eq. 13 is in general a full symmetric
(in the case of linear elasticity) matrix of the form

$$k_e = \begin{bmatrix} k_{e|11} & k_{e|12} & k_{e|13} & k_{e|14} & k_{e|15} & k_{e|16} & k_{e|17} & k_{e|18} \\ k_{e|12} & k_{e|22} & k_{e|23} & k_{e|24} & k_{e|25} & k_{e|26} & k_{e|27} & k_{e|28} \\ k_{e|13} & k_{e|23} & k_{e|33} & k_{e|34} & k_{e|35} & k_{e|36} & k_{e|37} & k_{e|38} \\ k_{e|14} & k_{e|24} & k_{e|34} & k_{e|44} & k_{e|45} & k_{e|46} & k_{e|47} & k_{e|48} \\ k_{e|15} & k_{e|25} & k_{e|35} & k_{e|45} & k_{e|55} & k_{e|56} & k_{e|57} & k_{e|58} \\ k_{e|16} & k_{e|26} & k_{e|36} & k_{e|46} & k_{e|56} & k_{e|66} & k_{e|67} & k_{e|68} \\ k_{e|17} & k_{e|27} & k_{e|37} & k_{e|47} & k_{e|57} & k_{e|67} & k_{e|77} & k_{e|78} \\ k_{e|18} & k_{e|28} & k_{e|38} & k_{e|48} & k_{e|58} & k_{e|68} & k_{e|78} & k_{e|88} \end{bmatrix}. \quad (14)$$

140 *3.2. Formulation of the ERR with respect to FEM variables*

4. Convergence analysis

4.1. Analytical considerations

4.2. Numerical results

5. Conclusions & Outlook

145 Acknowledgements

Luca Di Stasio gratefully acknowledges the support of the European School of Materials (EUSMAT) through the DocMASE Doctoral Programme and the European Commission through the Erasmus Mundus Programme.

References

- 150 [1] M. Comninou, An overview of interface cracks, *Engineering Fracture Mechanics* 37 (1) (1990) 197–208. doi:10.1016/0013-7944(90)90343-f.
- [2] D. Hills, J. Barber, Interface cracks, *International Journal of Mechanical Sciences* 35 (1) (1993) 27–37. doi:10.1016/0020-7403(93)90062-y.
- [3] M. L. Williams, The stresses around a fault or crack in dissimilar media, 155 *Bulletin of the Seismological Society of America* 49 (2) (1959) 199.

- [4] J. Dundurs, Discussion: “edge-bonded dissimilar orthogonal elastic wedges under normal and shear loading” (bogy, d. b., 1968, ASME j. appl. mech., 35, pp. 460–466), Journal of Applied Mechanics 36 (3) (1969) 650. doi:10.1115/1.3564739.
- 160 [5] F. Erdogan, Stress distribution in a nonhomogeneous elastic plane with cracks, Journal of Applied Mechanics 30 (2) (1963) 232. doi:10.1115/1.3636517.
- [6] A. H. England, A crack between dissimilar media, Journal of Applied Mechanics 32 (2) (1965) 400. doi:10.1115/1.3625813.
- 165 [7] B. Malyshev, R. Salganik, The strength of adhesive joints using the theory of cracks, International Journal of Fracture Mechanics 1-1 (2). doi:10.1007/bf00186749.
URL <https://doi.org/10.1007/bf00186749>
- [8] M. Comninou, The interface crack, Journal of Applied Mechanics 44 (4)
170 (1977) 631. doi:10.1115/1.3424148.
URL <https://doi.org/10.1115/1.3424148>
- [9] A. H. England, An arc crack around a circular elastic inclusion, Journal of Applied Mechanics 33 (3) (1966) 637. doi:10.1115/1.3625132.
- 175 [10] A. Perlman, G. Sih, Elastostatic problems of curvilinear cracks in bonded dissimilar materials, International Journal of Engineering Science 5 (11) (1967) 845–867. doi:10.1016/0020-7225(67)90009-2.
- [11] M. Toya, A crack along the interface of a circular inclusion embedded in an infinite solid, Journal of the Mechanics and Physics of Solids 22 (5) (1974) 325–348. doi:10.1016/0022-5096(74)90002-7.
- 180 [12] F. París, J. C. Caño, J. Varna, The fiber-matrix interface crack — a numerical analysis using boundary elements, International Journal of Fracture 82 (1) (1996) 11–29. doi:10.1007/bf00017861.

- [13] G. R. Irwin, Fracture, in: Elasticity and Plasticity / Elastizität und Plastizität, Springer Berlin Heidelberg, 1958, pp. 551–590. doi:10.1007/978-3-642-45887-3_5.
- [14] J. C. D. Caño, F. París, On stress singularities induced by the discretization in curved receding contact surfaces: a bem analysis, International Journal for Numerical Methods in Engineering 40 (12) (1997) 2301–2320. doi:10.1002/(sici)1097-0207(19970630)40:12<2301::aid-nme166>3.0.co;2-8.
- [15] J. Varna, F. París, J. C. Caño, The effect of crack-face contact on fiber/matrix debonding in transverse tensile loading, Composites Science and Technology 57 (5) (1997) 523–532. doi:10.1016/s0266-3538(96)00175-3.
- [16] F. París, E. Correa, V. Mantič, Kinking of transversal interface cracks between fiber and matrix, Journal of Applied Mechanics 74 (4) (2007) 703. doi:10.1115/1.2711220.
- [17] E. Correa, E. Gamstedt, F. París, V. Mantič, Effects of the presence of compression in transverse cyclic loading on fibre–matrix debonding in unidirectional composite plies, Composites Part A: Applied Science and Manufacturing 38 (11) (2007) 2260–2269. doi:10.1016/j.compositesa.2006.11.002.
- [18] E. Correa, V. Mantič, F. París, Effect of thermal residual stresses on matrix failure under transverse tension at micromechanical level: A numerical and experimental analysis, Composites Science and Technology 71 (5) (2011) 622–629. doi:10.1016/j.compscitech.2010.12.027.
- [19] E. Correa, F. París, V. Mantič, Effect of the presence of a secondary transverse load on the inter-fibre failure under tension, Engineering Fracture Mechanics 103 (2013) 174–189. doi:10.1016/j.engfracmech.2013.02.026.

- 210 [20] E. Correa, F. París, V. Mantič, Effect of a secondary transverse load on the inter-fibre failure under compression, *Composites Part B: Engineering* 65 (2014) 57–68. doi:10.1016/j.compositesb.2014.01.005.
- [21] C. Sandino, E. Correa, F. París, Numerical analysis of the influence of a nearby fibre on the interface crack growth in composites under transverse
215 tensile load, *Engineering Fracture Mechanics* 168 (2016) 58–75. doi:10.1016/j.engfracmech.2016.01.022.
- [22] C. Sandino, E. Correa, F. París, Interface crack growth under transverse compression: nearby fibre effect, in: *Proceeding of the 18th European Conference on Composite Materials (ECCM-18)*, 2018.
- 220 [23] L. Zhuang, A. Pupurs, J. Varna, R. Talreja, Z. Ayadi, Effects of inter-fiber spacing on fiber-matrix debond crack growth in unidirectional composites under transverse loading, *Composites Part A: Applied Science and Manufacturing* 109 (2018) 463–471. doi:10.1016/j.compositesa.2018.03.031.
- 225 [24] J. Varna, L. Q. Zhuang, A. Pupurs, Z. Ayadi, Growth and interaction of debonds in local clusters of fibers in unidirectional composites during transverse loading, *Key Engineering Materials* 754 (2017) 63–66. doi:10.4028/www.scientific.net/kem.754.63.
- [25] L. Zhuang, R. Talreja, J. Varna, Transverse crack formation in unidirectional composites by linking of fibre/matrix debond cracks, *Composites Part A: Applied Science and Manufacturing* 107 (2018) 294–303.
230 doi:10.1016/j.compositesa.2018.01.013.
- [26] E. Rybicki, M. Kanninen, A finite element calculation of stress intensity factors by a modified crack closure integral, *Engineering Fracture Mechanics* 9 (4) (1977) 931–938. doi:10.1016/0013-7944(77)90013-3.
235
- [27] R. Krueger, Virtual crack closure technique: History, approach, and appli-

cations, Applied Mechanics Reviews 57 (2) (2004) 109. doi:10.1115/1.1595677.

[28] C. Sun, C. Jih, On strain energy release rates for interfacial cracks in bi-
material media, Engineering Fracture Mechanics 28 (1) (1987) 13–20. doi:
10.1016/0013-7944(87)90115-9.

URL [https://doi.org/10.1016/0013-7944\(87\)90115-9](https://doi.org/10.1016/0013-7944(87)90115-9)

[29] M. Manoharan, C. Sun, Strain energy release rates of an interfacial crack
between two anisotropic solids under uniform axial strain, Composites Sci-
ence and Technology 39 (2) (1990) 99–116. doi:10.1016/0266-3538(90)
90049-b.

URL [https://doi.org/10.1016/0266-3538\(90\)90049-b](https://doi.org/10.1016/0266-3538(90)90049-b)

[30] C. Sun, W. Qian, The use of finite extension strain energy release rates in
fracture of interfacial cracks, International Journal of Solids and Structures
34 (20) (1997) 2595–2609. doi:10.1016/s0020-7683(96)00157-6.

URL [https://doi.org/10.1016/s0020-7683\(96\)00157-6](https://doi.org/10.1016/s0020-7683(96)00157-6)

[31] Simulia, Providence, RI, USA, ABAQUS/Standard User’s Manual, Version
6.12 (2012).